BIOCHEMISTRY
including biophysical chemistry & molecular biology

Article

pubs.acs.org/biochemistry

Acetylation of Gly1 and Lys2 Promotes Aggregation of Human γD-Crystallin

Michael A. DiMauro,[§,#] Sandip K. Nandi,[†,#] Cibin T. Raghavan,[§,∥] Rajiv Kumar Kar,[⊥] Benlian Wang,[‡] Anirban Bhunia,[⊥] Ram H. Nagaraj,[*,§,∥] and Ashis Biswas[*,†]

[§]Department of Ophthalmology and Visual Sciences and [‡]Center for Proteomics and Bioinformatics, Case Western Reserve University School of Medicine, Cleveland, Ohio, United States

[†]School of Basic Sciences, Indian Institute of Technology Bhubaneswar, Odisha, India

[⊥]Department of Biophysics, Bose Institute, Kolkata, India

Supporting Information

ABSTRACT: The human lens contains three major protein families: α-, β-, and γ-crystallin. Among the several variants of γ-crystallin in the human lens, γD-crystallin is a major form. γD-Crystallin is primarily present in the nuclear region of the lens and contains a single lysine residue at the second position (K2). In this study, we investigated the acetylation of K2 in γD-crystallin in aging and cataractous human lenses. Our results indicated that K2 is acetylated at an early age and that the amount of K2-acetylated γD-crystallin increased with age. Mass spectrometric analysis revealed that in addition to K2, glycine 1 (G1) was acetylated in γD-crystallin from human lenses and in γD-crystallin acetylated *in vitro*. The chaperone ability of α-crystallin for acetylated γD-crystallin was lower than that for the nonacetylated protein. The tertiary structure and the microenvironment of the cysteine residues were significantly altered by acetylation. The acetylated protein exhibited higher surface hydrophobicity, was unstable against thermal and chemical denaturation, and exhibited a higher propensity to aggregate at 80 °C in comparison to the nonacetylated protein. Acetylation enhanced the GdnHCl-induced unfolding and slowed the subsequent refolding of γD-crystallin. Theoretical analysis indicated that the acetylation of K2 and G1 reduced the structural stability of the protein and brought the distal cysteine residues (C18 and C78) into close proximity. Collectively, these results indicate that the acetylation of G1 and K2 residues in γD-crystallin likely induced a molten globule-like structure, predisposing it to aggregation, which may account for the high content of aggregated proteins in the nucleus of aged and cataractous human lenses.

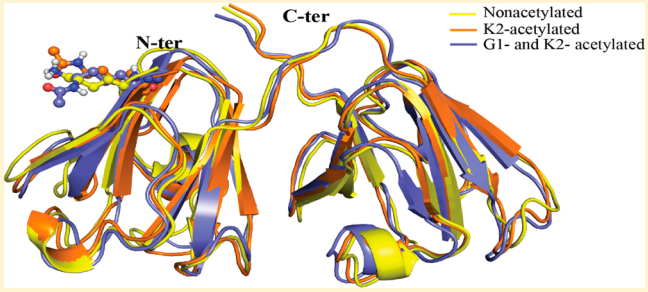

The mature lens is an avascular, soft, and transparent organ composed of a monolayer of epithelial cells that continually grows throughout life. The epithelial cells near the equatorial region undergo mitotic division, elongate, and then transform into fiber cells. During this elongation, the fiber cells accumulate high concentrations of crystallins (~300−450 mg/mL).[1] This concentrated, protein-rich material not only provides mechanical and structural stability to the eye lens but also contributes to its refractive properties and transparency.[2,3] Because protein turnover in the lens is minimal, crystallins must remain soluble and maintain their structure throughout the life span of an individual. However, with age, these lens proteins undergo several modifications, which result in the formation of insoluble protein aggregates. This protein aggregation or insolubility causes visible opacity and, thus, cataract formation during aging.

Three major crystallin protein families (α-, β-, and γ-crystallin) constitute greater than 90% of the total proteins of the lens, and α-crystallin constitutes ~50% of the total lens protein mass.[4] α-Crystallin is a large oligomeric protein composed of two subunits, αA- and αB-crystallin. In 1992, Horwitz first demonstrated that α-crystallin exhibited molecular chaperone activity.[5] By virtue of this property, α-crystallin is thought to prevent the aggregation of other lens proteins during aging and, thus, maintains lens transparency. β- and γ-Crystallins are the natural substrates of α-crystallin. These proteins function solely as structural proteins whose packing and interactions are optimized for the maintenance of eye lens transparency and refractivity.

The human lens contains five different γ-crystallins encoded by five different genes (γA, γB, γC, γD, and γS). γD-Crystallin is highly expressed in human lenses, in addition to γC- and γS-crystallins. Human γD-crystallin, which is a monomeric protein with a molecular mass of ~20 kDa, contains 173 amino acid residues.[6] This protein contains predominantly β-sheet structure, and its three-dimensional structure was elucidated by X-ray crystallography, revealing four Greek key motifs organized into two homologous domains.[7] Several posttranslational modifica-

Received: August 11, 2014
Revised: October 27, 2014
Published: October 30, 2014

dx.doi.org/10.1021/bi501004y | *Biochemistry* 2014, 53, 7269−7282

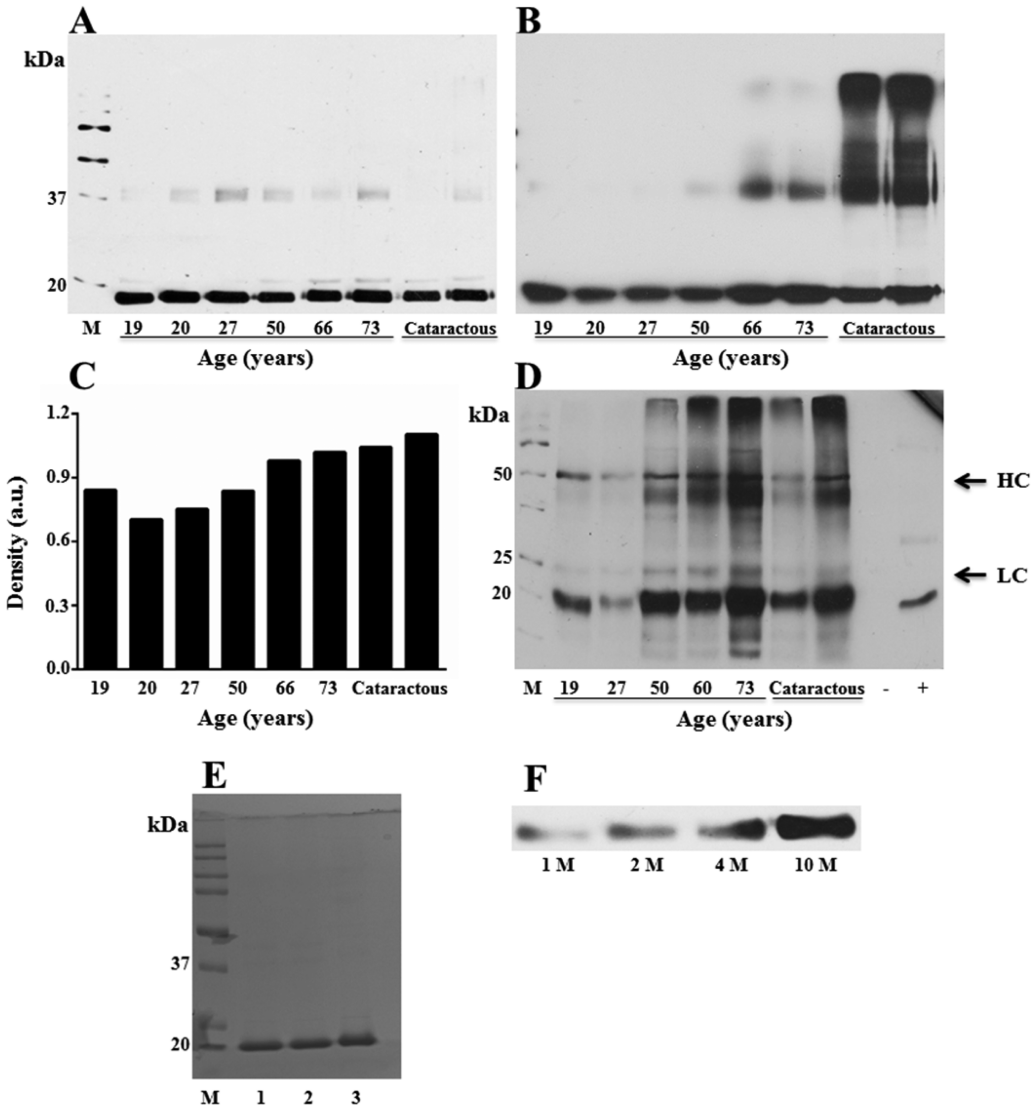

Figure 1. Detection of K2-acetylated γD-crystallin in the human lens. Western blot analysis of γD-crystallin and N^{ϵ}-acetyllysine-modified proteins in the human lens. Water-soluble human lens proteins were subjected to Western blot analysis using a monoclonal antibody against γD-crystallin (A). The membrane was stripped and reprobed using a monoclonal antibody against N^{ϵ}-acetyllysine (B). Densitometry of Western blot B is shown in C. Water-soluble human lens proteins were immunoprecipitated using a monoclonal antibody against γD-crystallin and were subjected to Western blot analysis using an antibody against N^{ϵ}-acetyllysine (D). The age of the donor lenses is shown below the lanes. M denotes the molecular weight markers. Arrows indicate the positions of the light (LC) and heavy chains (HC) of the antibody. The (−) denotes nonacetylated recombinant γD-crystallin; the (+) denotes *in vitro* acetylated recombinant γD-crystallin. SDS-PAGE of the purified γD-crystallin is shown in panel E. Lanes 1 and 2 are two preparations of γD-crystallin, and lane 3 is *in vitro* acetylated γD-crystallin. Western blot analysis of acetylated γD-crystallin using an antibody against N^{ϵ}-acetyllysine; acetylation was carried out using various molar excess concentrations of Ac_2O relative to lysine in γD-crystallin (F).

tions of human γD-crystallin have been reported in human lenses, among which include the oxidation of tryptophan (W156) and the deamidation of glutamine and asparagine (Q12, N49, and N160).[8−13] These modifications have been found to accumulate in cataractous lenses to a greater extent than in noncataractous, clear lenses.[13] In contrast, *S*-methylation of cysteine residues in human γD-crystallin was predominantly found in young clear lenses, which suggests that inhibition of disulfide bond formation due to this modification may play an important role in the long term survival of γD-crystallin against environmental stress.[14]

Acetylation is another important posttranslational modification found in human lens crystallins. Lapko et al. reported that the N-terminal glycine residue (the N-terminal methionine is naturally cleaved in γD-crystallin; thus, glycine becomes the N-terminal residue) of γD-crystallin is acetylated *in vivo*.[14] This N-terminal acetylation, which is a widespread phenomenon in eukaryotic cells, is mediated by N^{α}-acetyltransferase.[15] Acetylation of the ε-amino group of lysine is another modification. Lysine (K) acetylation is mediated by a lysine acetyltransferase (KAT), which transfers the acetyl group of acetyl-coenzyme A to the ε-amino group of the lysine residue of a protein.[16] The N-acetylation of lysine residues in proteins can be reversed by lysine deacetylase (KDAC).[17] Recently, we have identified that K70 and K99 in αA-crystallin, as well as K92 and K166 in αB-crystallin, are acetylated in the human lens.[18−20] Although human γD-crystallin contains only one lysine residue at position 2 (the numbering for the residues is based on the γD-crystallin crystal structure, PDB code: 1HK0),[7] this lysine acetylation has not been previously reported. Additionally, the impact of

dx.doi.org/10.1021/bi501004y | *Biochemistry* 2014, 53, 7269−7282

acetylation on the structure and aggregation of human γD-crystallin is unknown.

In this study, we have found that G1 and K2 are acetylated in γD-crystallin from human lenses. We found that such acetylation increases stress-induced aggregation of γD-crystallin and decreases its chaperoning by α-crystallin. Our biochemical, biophysical, and theoretical analyses provide the molecular basis for enhanced aggregation of the acetylated γD-crystallin.

MATERIALS AND METHODS

Dithiothreitol (DTT); 4,4′-dianilino-1,1′-binaphthyl-5,5′-disulfonic acid, dipotassium salt (bis-ANS); guanidium hydrochloride (GdnHCl); and ethylenediaminetetraacetic acid, disodium salt dehydrate (EDTA) were obtained from Sigma Chemical Co. (St. Louis, MO). 5,5′-Dithiobis(2-nitrobenzoic acid) (DTNB) was obtained from Sisco Research Laboratories, India. α_L-Crystallin was purified from bovine eye lenses, as previously described.[21] All other chemicals were of analytical grade.

Detection of N^{ε}-Acetyllysine in γD-Crystallin of the Human Lens. The ages of the analyzed noncataractous lenses are shown in Figure 1. The cataractous lenses were obtained from 65- to 75-year-old donors. Each lens was processed through homogenization, centrifugation, and sonication to obtain the water-soluble protein, as previously described.[18] Water-soluble proteins (20 μg from each lens) were analyzed on a 12% denaturing gel, transferred to a nitrocellulose membrane, and probed with a monoclonal antibody against human γD-crystallin (1:2500 dilution, Santa Cruz Biotechnology, Dallas, TX) and an HRP-conjugated goat antimouse IgG (1:5000 dilution, Promega, Madison, WI). The immunoreactivity was identified using the SuperSignal West Pico Chemiluminescent Substrate (Thermo Scientific, Waltham, MA). The membrane was reprobed using a monoclonal antibody against N^{ε}-acetyllysine (1:2500 dilution, Cell Signaling Technologies, Danvers, MA).

The water-soluble protein samples were also immunoprecipitated using a monoclonal antibody against human γD-crystallin by adding 5 μL of the antibody to 500 μg of protein from various lenses followed by incubation with mixing for 4 h at 37 °C. Twenty microliters of Protein A/G Agarose (Santa Cruz Biotechnology) was then added to each sample and incubated with mixing at 4 °C overnight. The samples were centrifuged at 1000*g* for 5 min at 4 °C. Pellets were washed on ice three times with a cell lysis buffer (Cell Signaling Technologies) and resuspended in 30 μL of 2× SDS sample buffer. The samples were subsequently analyzed on a 12% denaturing gel and probed for N^{ε}-acetyllysine as previously described.

Cloning, Expression, and Purification of Human γD-Crystallin. The human γD-crystallin in pET-3d plasmid was a kind gift from Dr. Ajay Pande of the University at Albany. The bacterial expression and purification of γD-crystallin were performed using previously described methods[22] with minor modifications. Briefly, the amplified PCR product was recloned into a pET-23d vector at the *Nco*I/*Bam*HI restriction sites in which the *Nde*I site had been replaced with an *Nco*I site. The resultant DNA was transformed into BL21(DE3) pLysS cells to overexpress the recombinant protein. When the culture reached its target density of OD ≈ 0.8 (OD 600 nm), the recombinant proteins were overexpressed in *E. coli* BL21(DE3) pLysS cells by induction with 500 μM IPTG. The bacterial pellet obtained after centrifugation at 5000*g* was suspended in 50 mM Tris, pH 8.0, containing 50 mM NaCl, 2 mM EDTA, and 10 μL/mL of a protease inhibitor cocktail (Sigma, Cat# P8849). Lysozyme was added to the cell suspension at 0.3 mg/mL and incubated for 10 min at 37 °C followed by sonication on ice at 30% amplitude and duty cycle = 40. To the resulting cell lysate, 1.0 μL of benzonase nuclease (Sigma-Aldrich, Cat#E1014) was then added and incubated at 37 °C in a shaker for 20 min, which was followed by the addition of sodium deoxycholate at 1.0 mg/mL and another incubation for 10 min at 37 °C. DTT was then added to the lysate at a 5 mM concentration and incubated for 10 min at 37 °C. The cell lysate was centrifuged at 20000*g* for 30 min at 4 °C. DNA in the lysate was precipitated by adding 0.2% polyethylenimine followed by centrifugation at 20000*g* for 15 min. Ammonium sulfate was added to the lysate to reach 60% saturation; the protein solution was then left at 4 °C overnight and centrifuged at 20000*g* for 5 min. The resulting pellet was suspended in 50 mM sodium phosphate buffer, pH 7.4, containing 150 mM NaCl and 5 mM DTT, and it was centrifuged at 20000*g* for 5 min. The supernatant was passed through a 10 kDa MWCO filter. The retenate from the filtration was dialyzed for 48 h against PBS with 0.2 mM EDTA before loading onto a Sephacryl S-200 HR column. Elution was carried out using 50 mM sodium phosphate buffer, pH 7.4, containing 5 mM DTT. Fractions of 3.0 mL were collected, and their OD at 280 nm was recorded. SDS-PAGE of the fractions was carried out to detect γD-crystallin; fractions containing γD-crystallin were pooled and dialyzed for 24 h at 4 °C against PBS with 0.2 mM EDTA.

***In vitro* Acetylation of Recombinant Human γD-Crystallin.** Acetylation of human recombinant γD-crystallin was performed as previously described with minor modifications.[18] Acetic anhydride (Ac_2O) was prepared in dioxane to a final concentration of 50 mM and added to 500 μg of recombinant γD-crystallin over a period of 1 h to obtain K2 at Ac_2O molar ratios of 1:0, 1:1, 1:2, 1:4, and 1:10, with the pH controlled at 7.4 using diluted NH_4OH as necessary. Samples were dialyzed overnight against PBS. We dialyzed nonacetylated and acetylated γD-crystallin against suitable buffers prior to each biophysical and biochemical assay.

Identification of Acetylation Sites in Human γD-Crystallin Using Mass Spectroscopy. Water-soluble γD-crystallin (500 μg) isolated from a 73-year-old human lens was immunoprecipitated using a γD-crystallin antibody (5 μL), as previously described, and the resultant gel pellet was dissolved in the sample buffer and subjected to SDS-PAGE analysis. Recombinant γD-crystallin that had been acetylated as previously described (with a 10 molar excess of Ac_2O) was also subjected to SDS-PAGE analysis. SDS-PAGE gel bands containing γD-crystallin were cut into small pieces and destained with 50% acetonitrile in 100 mM ammonium bicarbonate followed by dehydration in 100% acetonitrile and then dried in a SpeedVac centrifuge. Prior to overnight in-gel trypsin digestion, the protein was chemically reduced using 20 mM DTT at room temperature for 1 h and alkylated with 50 mM iodoacetamide in 50 mM ammonium bicarbonate for 30 min in the dark. Proteolytic peptides were extracted from gels using 50% acetonitrile in 5% formic acid and then resuspended in 0.1% formic acid after being completely dried under a vacuum. The analysis of the resultant peptides was performed using an Orbitrap Elite hybrid mass spectrometer (Thermo Scientific, San Jose, CA, USA) equipped with a Waters nanoACQUITY UPLC system (Waters, Taunton, MA, USA). Spectra were recorded using data-dependent methods that involved an alternative full scan followed by 20 MS/MS scans. The data were analyzed using Mascot Daemon (Matrix Science, Boston, MA) at a setting of 10 ppm for parent ions and 0.8 Da for product ions. Carbamidomethylation of Cys (C) residues were set as fixed modifications, and oxidation of

dx.doi.org/10.1021/bi501004y | *Biochemistry* 2014, 53, 7269−7282

Met and acetylation of N-terminal G1 and K2 residues were set as variable modifications. Acetylation sites were further verified by manual examination of each tandem mass spectrum.

Circular Dichroism (CD) Measurements. Far-UV CD spectra were measured at 25 °C using a Chirascan-plus spectrometer (Applied Photophysics, UK). Spectra were collected from 195 to 260 nm using a cylindrical quartz cell with a 1 mm path length. Proteins (0.2 mg/mL) were dissolved in 10 mM phosphate buffer, 5 mM DTT, and 1 mM EDTA (pH 7.0). The reported spectra are the average of five scans. Spectra were analyzed for secondary structure content using the CONTILL curve-fitting program.[23] The near-UV CD spectra were measured at 25 °C using an identical spectropolarimeter. The spectra were measured with a 1.0 mg/mL protein solution in 10 mM phosphate buffer, 5 mM DTT, and 1 mM EDTA (pH 7.0). The reported spectra are the average of five scans.

Intrinsic Tryptophan Fluorescence Measurements. The intrinsic tryptophan fluorescence spectra of the proteins (0.025 mg/mL) in 10 mM phosphate buffer, 5 mM DTT, and 1 mM EDTA (pH 7.0) at 25 °C were recorded using a FluoroMax-4P spectrofluorometer (Horiba Jobin Mayer, USA). The excitation wavelength was set to 295 nm, and the emission spectra were recorded between 310 and 400 nm. The data were collected at 0.5 nm wavelength resolution.

Bis-ANS Fluorescence Experiment. Bis-ANS (10 μM) was added to nonacetylated and acetylated γD-crystallin (0.05 mg/mL in 10 mM phosphate buffer, 5 mM DTT, and 1 mM EDTA [pH 7.0]), and the mixture was incubated for 1 h at 25 °C. Fluorescence emission spectra were recorded between 450 and 600 nm using an excitation wavelength of 390 nm. The excitation and emission band passes were 2.5 and 5 nm, respectively. The data were collected at 0.5 nm wavelength resolution.

Quantification of Sulfhydryl Groups. Proteins at a concentration of 0.4 mg/mL in 50 mM phosphate buffer containing 1 mM EDTA (pH 7.4) and DTNB solution were added to yield a protein to DTNB molar ratio of 1:7. Following the addition of DTNB, the exposure of thiol groups was monitored by measuring the absorbance at 412 nm at 25 °C as a function of time in a PerkinElmer spectrophotometer fitted with a thermostatic cell holder and an electronic temperature control. A molar extinction coefficient of 14 150 M^{-1} cm^{-1} for the thionitrophenylate anion at 412 nm was used to calculate the amount of sulfhydryl (free -SH) groups present in γD-crystallin samples. To confirm the thiol specificity, we also performed an identical experiment using *Mycobacterium leprae* HSP18, which lacks cysteine residues.

Estimation of Structural Stability. *(a). Chemical Denaturation.* The structural stability of nonacetylated and acetylated human γD-crystallin was determined using an equilibrium chemical denaturation experiment. Both proteins (0.025 mg/mL in 10 mM phosphate buffer, 5 mM DTT and 1 mM EDTA [pH 7.0]) were individually incubated with various concentrations of GdnHCl (0−7 M) for 18 h at 37 °C. Intrinsic tryptophan fluorescence spectra of all samples were recorded between 310 and 400 nm using an excitation wavelength of 295 nm. The equilibrium unfolding profile was fit according to a three-state model.[18,20,24]

(b). Thermal Denaturation Monitoring the Intrinsic Tryptophan Fluorescence. The structural stability of nonacetylated and acetylated human γD-crystallin was also determined by monitoring the changes in the maximum emission wavelength (λ_{max}) of the intrinsic tryptophan fluorescence in a FluoroMax-4P spectrofluorometer equipped with a temperature-controlled water bath. The change in λ_{max} was recorded stepwise between 25 and 90 °C in a quartz cell, allowing the samples to equilibrate at each temperature for 2 min. The data were recorded at intervals of 2 °C. A protein concentration of 0.025 mg/mL in 10 mM phosphate buffer, 5 mM DTT, and 1 mM EDTA (pH 7.0) was used. The raw data were fitted to a two-state model, and the fitting results are indicated by solid lines.[24] The midpoint transition, or T_m, was calculated using sigmoidal analysis.[24]

(c). Thermal Denaturation Using far-UV CD Spectroscopy. The structural stability of nonacetylated and acetylated human γD-crystallin was also determined using thermally induced unfolding experiments in a Chirascan-plus spectrometer (Applied Photophysics, Leatherhead, UK) equipped with a Peltier system. The change in ellipticity at 218 nm was recorded stepwise between 25 and 90 °C in a quartz cell with a path length of 2 mm, allowing the samples to equilibrate at each temperature. The heating rate was set to 0.5 °C/min. The data were recorded at intervals of 2 °C. A protein concentration of 0.1 mg/mL in 10 mM phosphate buffer, 5 mM DTT, and 1 mM EDTA (pH 7.0) was used. The values for the fraction unfolded (α_U) for both proteins were calculated using the following equation:

$$\alpha_U = \frac{\theta_F - \theta_t}{\theta_F - \theta_U} \quad (1)$$

where θ_F is the ellipticity value at 25 °C for completely folded or native protein, θ_t is the observed ellipticity value at any temperature between 25 and 90 °C, and θ_U is the ellipticity value at 90 °C for the completely denatured or unfolded state. The T_m was calculated using sigmoidal analysis as previously described.[24]

Kinetics of Unfolding/Refolding. The time course of unfolding of nonacetylated and acetylated γD-crystallin in 5.5 M GdnHCl, 10 mM phosphate buffer, 5 mM DTT, and 1 mM EDTA (pH 7.0) was monitored by fluorescence emission at 355 nm using an excitation wavelength of 295 nm in a FluoroMax-4P spectrofluorometer. Protein at a concentration of 100 μg/mL was injected into the cuvette, yielding a final protein concentration of 10 μg/mL at two different temperatures (25 and 37 °C), with constant stirring. Fluorescence was monitored until no further changes were observed. Each unfolding experiment was performed in triplicate.

Refolding experiments were performed in an analogous fashion. Protein (100 μg/mL) that had been incubated in 5.5 M GdnHCl, 10 mM phosphate buffer, 5 mM DTT, and 1 mM EDTA (pH 7.0) at two different temperatures (25 and 37 °C) for 5 h was subsequently injected into 0.5 M GdnHCl in an identical buffer. The final GdnHCl concentration was 1.0 M, and the final protein concentration was 10 μg/mL.

***In Vitro* Aggregation Assay.** Nonacetylated and acetylated γD-crystallin (0.1 mg/mL) in 10 mM phosphate buffer, 5 mM DTT, and 1 mM EDTA (pH 7.0) were incubated at 80 °C. Light scattering at 400 nm was monitored for 1 h in the kinetic mode. Thermal aggregation of both proteins was also performed in the presence of 0.075 or 0.1 mg/mL α_L-crystallin.

Adaptive Poisson−Boltzmann Solver (APBS). The crystal structure of human γD-crystallin was obtained from the Protein Data Bank (PDB code: 1HK0).[7] Acetylation of G1 and K2 was considered when analyzing the bond order, overlapping atoms, and missing hydrogen atoms. The nonacetylated and acetylated γD-crystallin were further optimized by reorienting the hydroxyl groups and amide groups of Asn and Gln to define

dx.doi.org/10.1021/bi501004y | *Biochemistry* 2014, 53, 7269−7282

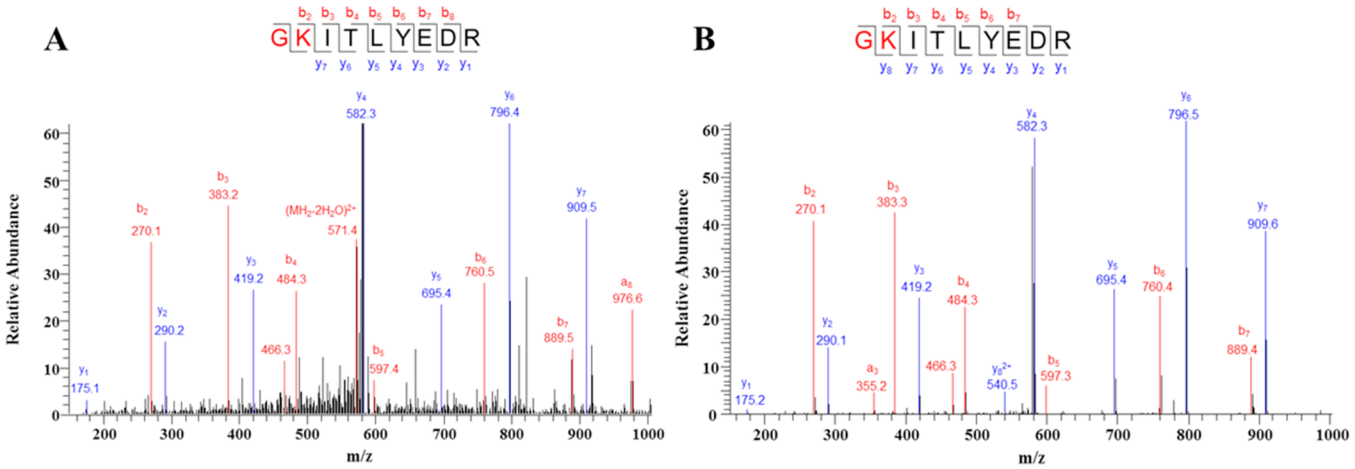

Figure 2. Mass spectrometric detection of acetylation at G1 and K2 in human γD-crystallin. Tandem mass spectra of γD-crystallin from a 73-year-old human lens (A) and *in vitro* acetylated γD-crystallin (B). The precursor ion of 589.81 (2+) that indicates a mass shift of +84 Da compared with the unmodified peptide is shown. The mass shift of +42 Da was observed at y8, but not y-series ions from y1 to y7, which indicated acetylation of K2. The mass shift of +84 Da was observed on the precursor ion, as well as b-series ions from b2 to b7, which suggested acetylation of K2 and G1.

the hydrogen bonding network. In addition, we also considered the appropriate orientation and states for the His residues of both proteins. The macro-model was subjected to minimization in the Protein Preparation Wizard (Schrödinger Suite) using the OPLS_2005[25] force field up to a maximum deviation of 0.8 Å. Final energy minimization of the protein macro-models was performed with 3500 steps, employing the Polak-Ribiere conjugate gradient algorithm, which iterates the energy minimization scheme every 3N steps. The energy minimized conformations were used to generate *pqr files* using the PDB 2PQR server.[26] All computations required to evaluate the electrostatic properties were performed using a plugin option of PyMOL *v1.2r3pre*. Visualization of the electrostatic isosurfaces was contoured at ±0.37 kT/e for positive and negative isosurfaces, respectively.

Molecular Dynamics (MD) Simulation. The structural behavior of the acetylated and nonacetylated γD-crystallin was further examined in solvent conditions using molecular dynamics simulations. An entire MD simulation was performed using Desmond utilizing the OPLS_2005 force field. Acetylation at K2 and G1 was manually introduced using the edit option in Maestro. Simulations using an equal time scale were performed for both the nonacetylated and the acetylated models of γD-crystallin. All of the hydrogen bonds were constrained using the M-SHAKE algorithm,[27] with an integration frequency of a 2 fs time step. A RESPA integrator[28] was employed with a 6 fs time step for long-range Coulomb interactions; electrostatic interactions were computed using the particle-mesh Ewald method with a cubic-β spline and a grid spacing of 1 Å. As a microcanonical system, an NPT ensemble was set up to execute the simulation at 1 bar pressure and a constant temperature of +27 °C (300 K). The temperature and pressure of the system was maintained employing Langevin dynamics and the Nosè-Hoover method. All of the models were solved using TIP3P water models with a 10-Å edge length in the orthorhombic boundary conditions. Appropriate quantities of counterions were added for neutralization. Initially, the systems were subjected to energy minimization with 4000 steps of steepest descent integration to avoid steric clashes between the atoms. The remaining protocol of energy minimization and equilibration was adopted from the default protocol in the Desmond MD simulation system (Desmond Molecular Dynamics System, version 3.4 (2013) D. E. Shaw Research, New York, NY. Maestro-Desmond Interoperability Tools, version 3.4, (2013) Schrodinger, New York, NY). All of the images were rendered using the PyMOL software.

Statistics. The data are presented as the means ± SD of the number of experiments indicated in the figure legends. The data were analyzed using the StatView software (SAS Institute Inc., Cary, NC). Statistical significance among the groups was determined using an analysis of variance, and $p < 0.05$ was considered significant.

RESULTS AND DISCUSSION

In the human lens γ-crystallin subtypes, γC, γD, and γS share approximately 80% amino acid sequence homology (Figure S1 of the Supporting Information). The N-terminal methionine residue that is incorporated during the translation initiation step has been found to be cleaved from all three of these γ-crystallins.[11,29] Furthermore, multiple sequence alignment of these γ-crystallins indicates that K2 is conserved among these three proteins (Figure S1 of the Supporting Information). Interestingly, Park et al. identified acetylation of this conserved lysine residue in γS-crystallin of the human lens.[9] We hypothesized that acetylation of K2 also occurs in human γD-crystallin. Recently, we demonstrated that lysine acetylation in α-crystallin enhanced its chaperone function.[18] In another study, we demonstrated that K92 acetylation improved the chaperone and antiapoptotic properties of human αB-crystallin.[20] Based on these observations, we hypothesized that acetylation could alter the structure, stability and aggregation properties of human γD-crystallin.

Western blot analysis using monoclonal antibodies against human γD-crystallin and N^{ϵ}-acetyllysine exhibited distinct immunoreactivity at approximately 20 kDa and 37 kDa in human lenses (Figure 1A,B). Furthermore, the total proteins bearing N^{ϵ}-acetyllysine increased with age (Figure 1B,C). To further confirm K2 acetylation in γD-crystallin, we immunoprecipitated γD-crystallin from human lenses and probed by Western blot analysis using an antibody against N^{ϵ}-acetyllysine. As shown in Figure 1D, N^{ϵ}-acetyllysine was present in γD-crystallin in all of the lenses. These results also indicated that K2 in γD-crystallin is acetylated at an early age and that this

dx.doi.org/10.1021/bi501004y | *Biochemistry* 2014, 53, 7269−7282

Table 1. Detection of Acetylated Amino Acids in Human γD-Crystallin

sequence	M_r (expt)	M_c (calc)	error (ppm)	modified site	mass shift (Da)	samples	
						in vitro	*in vivo*
GKITLYEDR	1093.5742	1093.5768	−2	none		X	X
GKITLYEDR	1135.5856	1135.5873	−1	protein N-terminus	+42.0106	X	X
GKITLYEDR	1177.5962	1177.5979	−1	protein N-terminus and K2	+84.0212	X	X

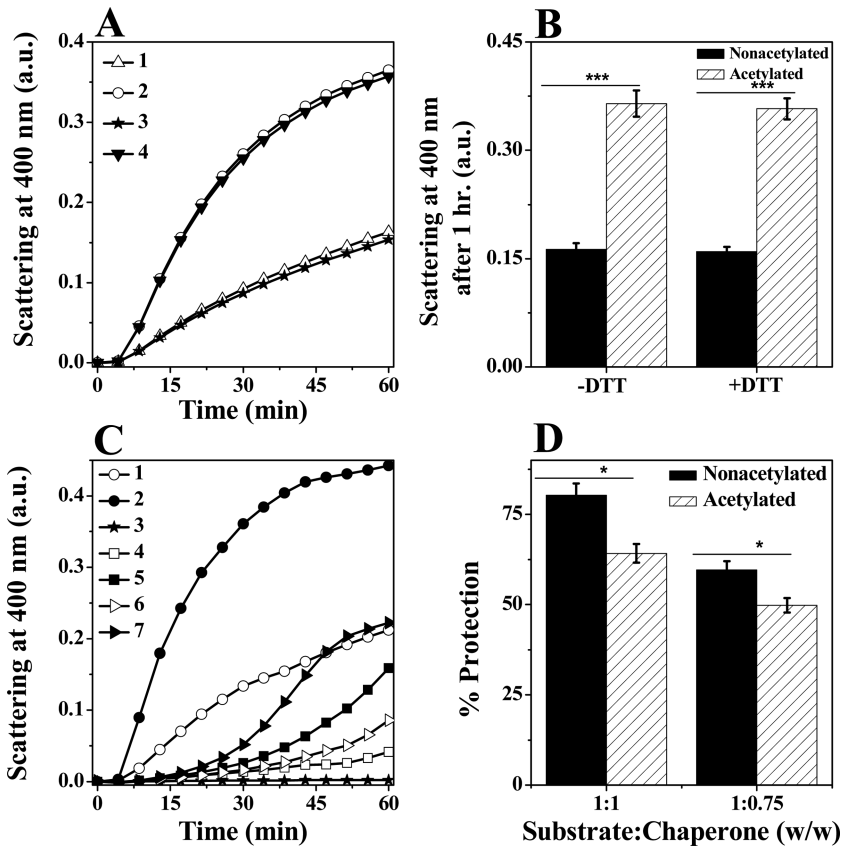

Figure 3. Acetylated γD-crystallin is more prone to thermal aggregation and less protected by α_L-crystallin. (A) Time-course aggregation of nonacetylated and acetylated human γD-crystallin at 80 °C. The samples were prepared in 10 mM phosphate buffer containing 1 mM EDTA (pH 7.0). 1: Nonacetylated; 2: acetylated; 3: nonacetylated with 5 mM DTT; and 4: acetylated with 5 mM DTT. The protein concentration was 0.1 mg/mL. (B) Scattering values of both proteins during thermal aggregation after 1 h. (C) Time-course aggregation of nonacetylated and acetylated γD-crystallin at 80 °C in the presence/absence of α_L-crystallin. The samples were prepared in 10 mM phosphate buffer containing 5 mM DTT and 1 mM EDTA (pH 7). The concentration of both γD-crystallin proteins was 0.1 mg/mL. 1: Nonacetylated; 2: acetylated; 3: α_L-crystallin alone; 4: nonacetylated + α_L-crystallin (1:1) (w/w); 5: acetylated + α_L-crystallin (1:1) (w/w); 6: nonacetylated + α_L-crystallin (1:0.75) (w/w); and 7: acetylated + α_L-crystallin (1:0.75)(w/w). (D) Percent protection of nonacetylated and acetylated γD-crystallin by α_L-crystallin during thermal aggregation after 1 h. Bars represent the means ± SD of three independent experiments. *p < 0.05 and ***p < 0.0005.

acetylation increased with age. Furthermore, we observed acetylation of γD-crystallin in cataractous lenses (Figure 1D).

SDS-PAGE of the recombinant γD-crystallin indicated that it was pure (Figure 1E). We then acetylated the purified γD-crystallin *in vitro* using Ac_2O. This modification did not result in cross-linking of the protein (Figure 1E, lane 3). Acetylation of recombinant γD-crystallin was achieved using different molar ratios of lysine to Ac_2O (considering one lysine residue per molecule of γD-crystallin). Western blot analysis using the N^{ϵ}-acetyllysine antibody indicated acetylation of γD-crystallin, and the intensity of the band increased as the concentration of Ac_2O increased (Figure 1F).

We further verified the acetylation sites in human γD-crystallin using mass spectrometry. Both γD-crystallin from a 73-year-old lens (Figure 2A) and *in vitro* acetylated γD-crystallin (Figure 2B) exhibited similar tandem mass patterns in the modified peptides (the sequence coverages for the two proteins were 94 and 99%, respectively). The N-terminal peptide GKITLYEDR of the protein was observed in both the unmodified and the modified forms with mass shifts of +42 Da and +84 Da (Table 1), indicating that in addition to K2 acetylation, G1 was acetylated in both the *in vivo* and the *in vitro* samples.

In the human lens, crystallins undergo various modifications.[8,30] Several studies have attempted to understand the effect of these modifications on the structure and function of crystallins.[18,31−34] For γD-crystallin, Flaugh et al. demonstrated that deamidation of glutamine destabilizes the protein by lowering the kinetic barrier to unfolding.[35] Schafheimer and King demonstrated that UVA/UVB radiation induced photoaggregation of γD-crystallin *in vitro*.[36] Therefore, to determine how acetylation affects γD-crystallin, we first examined the aggregation profiles of nonacetylated and acetylated γD-

dx.doi.org/10.1021/bi501004y | *Biochemistry* 2014, 53, 7269−7282

crystallin. The acetylated γD-crystallin exhibited a 2-fold increase in thermal aggregation in comparison to the nonacetylated protein (Figure 3A,B). The aggregation profiles of the nonacetylated and acetylated proteins remained unaltered in the presence of DTT (Figure 3A,B), suggesting that disulfide formation was not responsible for the greater aggregation of the acetylated protein. We then determined whether the ability of α-crystallin to suppress thermal aggregation was altered by acetylation of γD-crystallin. Heat-induced γD-crystallin aggregation profiles in the absence or presence of α-crystallin are shown in Figure 3C,D. α-Crystallin efficiently inhibited the aggregation of γD-crystallin (∼80%) at a chaperone to substrate ratio of 1:1 (w/w); however, acetylation decreased the chaperone efficiency by 20%. Similar results were obtained at a chaperone to substrate ratio of 0.75:1 (w/w). Under these assay conditions, α-crystallin did not aggregate (Figure 3C, trace 3). These results suggested that acetylation of G1 and K2 in human γD-crystallin enhanced its aggregation under thermal stress. The decreased chaperone function of α-crystallin for the acetylated protein further suggested that acetylation of γD-crystallin could lead to its aggregation in aging and cataractous lenses.

We have previously reported that acetylation of α-crystallin perturbed its structure.[18,32,33] To verify whether a similar structural perturbation occurred in γD-crystallin, we probed the structure by monitoring the intrinsic tryptophan fluorescence, in addition to using near- and far-UV CD spectroscopy. Far-UV CD spectra of the nonacetylated and the acetylated proteins were nearly identical (Figure 4A). The spectra exhibited characteristics of a dominant β-sheet structure (minima at approximately 218 nm). Quantitative analysis of the far-UV CD spectra confirmed that γD-crystallin is a predominantly β-sheet protein (55% β-sheet and only 8% α-helix). These results further indicated that G1 and K2 acetylation did not perturb the secondary structure of γD-crystallin.

The near-UV CD spectra of γD-crystallin are shown in Figure 4B. The signal for tryptophan and tyrosine (greater than 270 nm) was different in the acetylated protein compared with the nonacetylated protein. Moreover, peaks for phenylalanine in the 250−270 nm region for the acetylated protein were found to differ in both intensity and position from those of the nonacetylated protein. These alterations suggested that G1 and K2 acetylation significantly perturbed the tertiary structure of γD-crystallin. The intrinsic tryptophan fluorescence spectra of the two proteins agreed with the near-UV results (Figure 4C). The λ_{max} for both the nonacetylated and the acetylated protein occurred at 327 nm, which suggested that the tryptophan residues are buried. However, the intrinsic tryptophan fluorescence of the acetylated protein was ∼10% higher than that of the nonacetylated protein, suggesting that acetylation perturbed the microenvironment of the tryptophan residues.

We also used molecular dynamics simulations to understand the fluctuations in different conformations of γD-crystallin. The superposition of the nonacetylated and acetylated model structures (Figure 5A) revealed that the overall globular conformation was identical in the two proteins. The relative architecture of the protein, which consists of antiparallel β-sheets, was well preserved in the acetylated form. These results correlated well with the far-UV CD spectra (Figure 4A), in which the spectral characteristics were found to be identical for the acetylated and nonacetylated proteins. All four tryptophan (W) residues (W42, W68, W131 and W157) were found to be buried in the conformational samplings (Figure 5B), which,

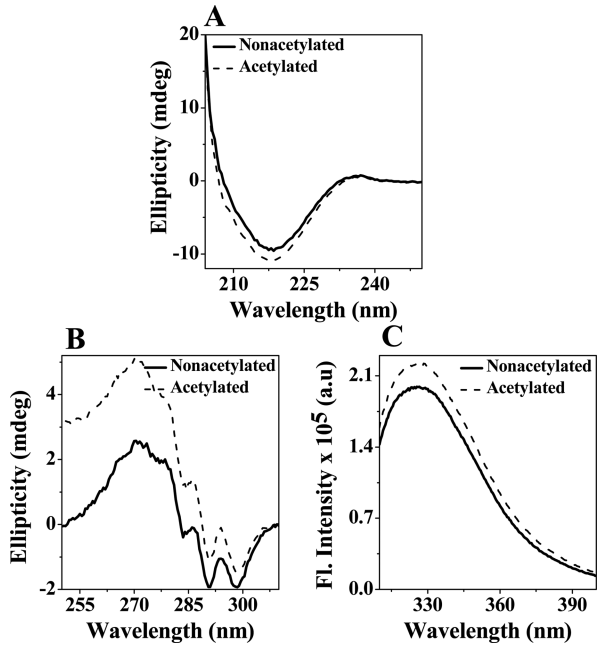

Figure 4. Acetylation perturbed only the tertiary structure of γD-crystallin. (A) Far-UV CD spectra of nonacetylated and acetylated human γD-crystallin. (B) Near-UV CD spectra of nonacetylated and acetylated human γD-crystallin. The concentrations of the protein samples used in far- and near-UV CD were 0.2 and 1.0 mg/mL, respectively. (C) Intrinsic tryptophan fluorescence spectra of nonacetylated and acetylated human γD-crystallin (0.025 mg/mL) were recorded from 310 to 400 nm. The excitation wavelength was 295 nm. Excitation and emission slit widths were 5 nm each. The data were collected at a 0.5 nm wavelength resolution. All assays were performed in 10 mM phosphate buffer containing 1 mM EDTA and 5 mM DTT (pH 7.0) at 25 °C.

again, fully agreed with our intrinsic tryptophan fluorescence results (Figure 4C).

Human γD-crystallin contains six cysteine residues. The crystal structure of human γD-crystallin (PDB code: 1HK0) indicated that all six cysteine residues exist in the reduced (−SH) form. Because acetylation perturbed the tertiary structure of γD-crystallin, we determined whether this perturbation was accompanied by alterations in the microenvironment of the cysteine residues. Upon reaction between DTNB and the −SH groups of the nonacetylated protein, 2-nitro-5-thiobenzoic acid (TNB) was formed, and, as a result of this adduct formation, an increase in the absorbance at 412 nm (A_{412}) with time was observed (Figure 6). This increase was significantly smaller in the acetylated protein. On the basis of these reactions, we estimated the DTNB-reactive sulfhydryl groups in the nonacetylated and acetylated protein to be 4.43 μM and 1.21 μM, respectively. To confirm whether changes in the DTNB assay were due to the alteration in the available free thiol moieties of cysteine residues, we performed the assay using the cysteine-lacking *Mycobacterium leprae* HSP18, which we have previously cloned and purified.[24] We did not observe a change in the absorbance value at 412 nm with time for HSP18. Collectively, these results confirmed that acetylation of γD-crystallin altered the microenvironment of cysteine residues in a manner that rendered them inaccessible for reaction with DTNB.

The X-ray crystal structure of human γD-crystallin indicated that cysteine (C) residues C18 and C78 are in close proximity and are therefore likely to form a disulfide bond. Heat map

dx.doi.org/10.1021/bi501004y | *Biochemistry* 2014, 53, 7269−7282

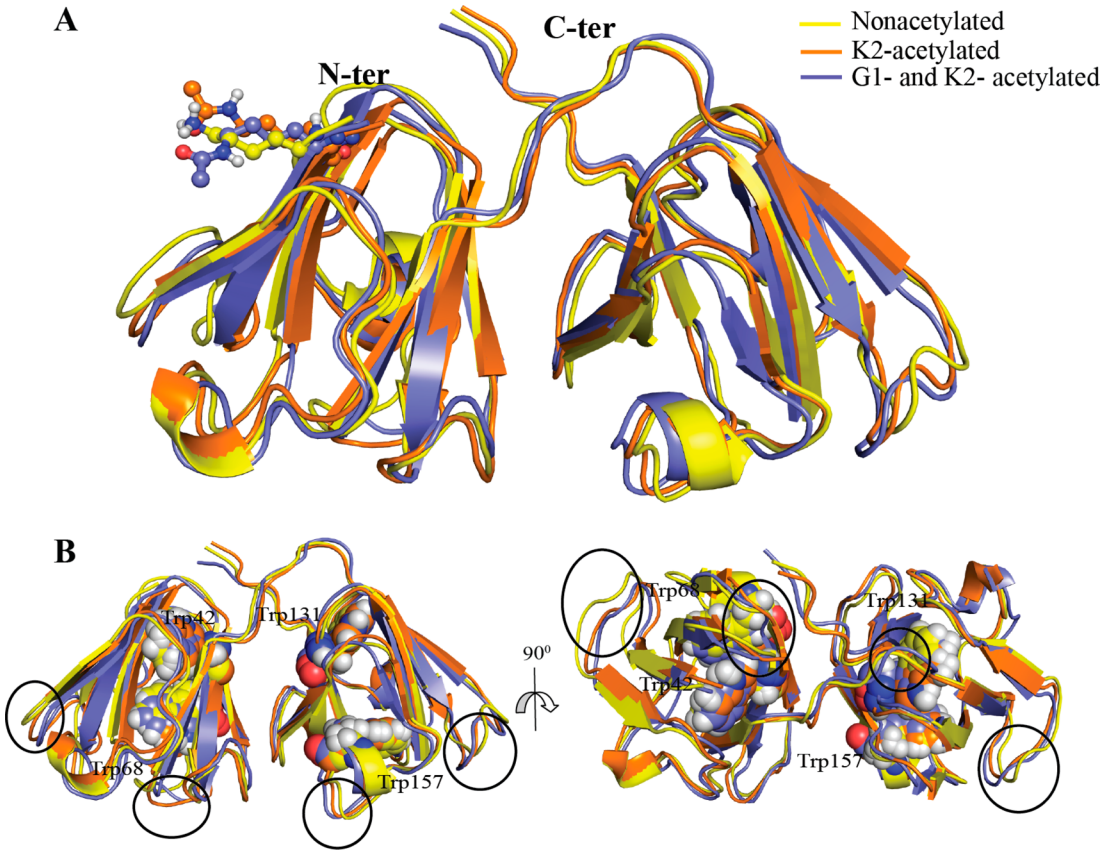

Figure 5. Conformational analysis of nonacetylated and acetylated γD-crystallin using molecular dynamics simulations. Molecular dynamics simulation results suggest that acetylation does not alter the secondary structure of γD-crystallin (A). Tryptophan residues in the nonacetylated (yellow), in the K2-acetylated (orange) and in the G1- and K2-acetylated γD-crystallin (blue) models are shown (B). The structures used for superposition are models from the top conformational cluster. All tryptophan residues were found to be buried within the globular core of the proteins. The "circled" portions in the panel B represents modulation in the structure/conformation of human γD-crystallin due to aceylation.

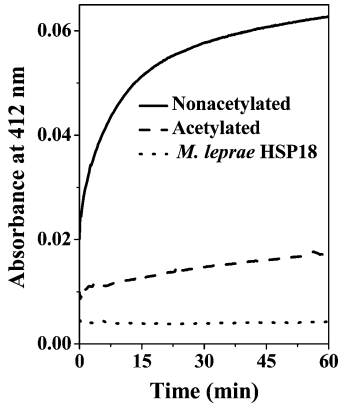

Figure 6. Acetylation alters the cysteine microenvironment in γD-crystallin. DTNB reaction kinetic profiles of nonacetylated and acetylated γD-crystallin at 25 °C. A protein concentration of 0.1 mg/mL in 50 mM phosphate buffer containing 1 mM EDTA (pH 7.4) was used. DTNB was used at a 7-fold molar excess of the protein. Absorbance was measured at 412 nm as a function of time. *Mycobacterium leprae* HSP18, which lacks cysteine residues, was used as a negative control.

analysis was performed based on the atomic information from molecular dynamics simulations to explore the energy minima points on the correlated projections. The *y*-axis was plotted by considering the RMSD for C18 and C78 as a collective variable. The interatomic distance between the sulfur atoms of both residues constituted the collective variable for the *x*-axis (Figure 7). An analysis of the structures representing the top cluster revealed the interatomic distance between C18 and C78 to be 5.1 Å in the nonacetylated, 4.2 Å in the K2-acetylated and 3.8 Å in the G1- and K2-acetylated proteins (Figure 7). The local minima were found to be much further to the right on the *x*-axis for the nonacetylated protein. In contrast, these minima were closer to the origin of the axis for the K2 acetylation model, suggesting that the two cysteine residues contained minimum energy and drew closer to each other. Interestingly, the minima was found to be even more conserved for the G1- and K2-acetylated protein, suggesting that the bond distance between C18 and C78 was reduced even further. These results correlate well with the *in vitro* thiol reactivity experiment (Figure 6) in which a significant reduction in the free −SH groups was observed for the acetylated protein. Collectively, acetylation of human γD-crystallin perturbed the cysteine microenvironments and brought the two cysteine residues within close proximity of each other.

In addition to these structural perturbations, we also probed the surface of nonacetylated and acetylated γD-crystallin. Molecular modeling based on the X-ray crystal structure was used to evaluate the changes in the surface electrostatics attributable to acetylation in human γD-crystallin. The acetylation was introduced at the G1 and K2 positions and analyzed using APBS. Prior to calculation, energy minimization of the macro-models was performed to ensure the correct positioning and orientation of each atom. The electrostatic isosurface revealed marked changes in the acetylated protein.

dx.doi.org/10.1021/bi501004y | *Biochemistry* 2014, 53, 7269−7282

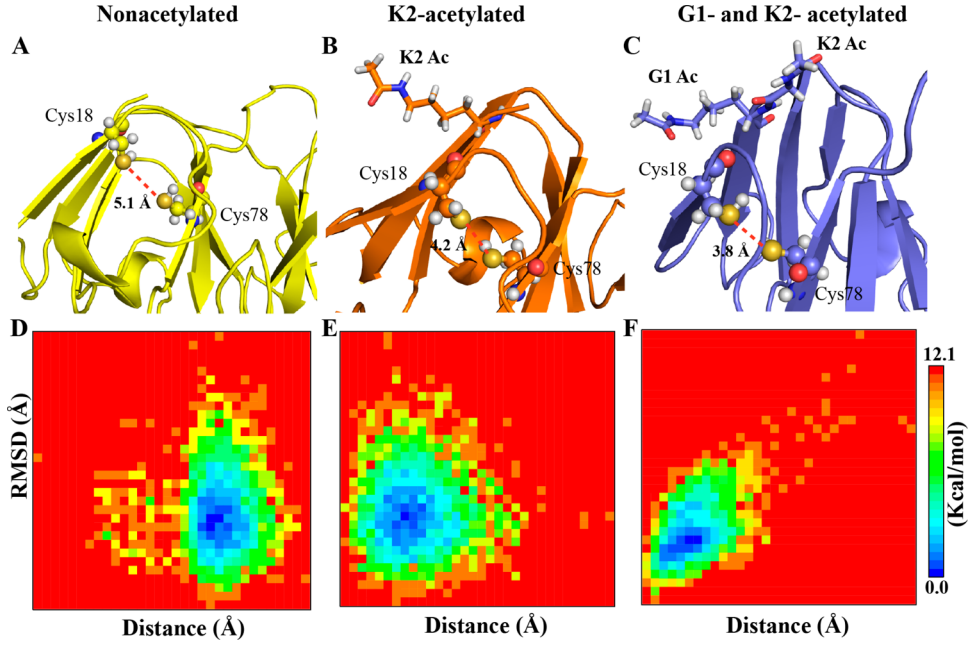

Figure 7. Orientation of thiol residues in nonacetylated and acetylated γD-crystallin. The relative distance between C18 and C78 in the nonacetylated (A), K2-acetylated (B), and G1- and K2-acetylated γD-crystallin (C) calculated from the top conformational cluster models. Heat map analysis for C18 and C78 of human γD-crystallin [nonacetylated (D), K2-acetylated (E), and G1- and K2-acetylated γD-crystallin (F)] was prepared using the root-mean-square deviation of C18 and C78 as collective variables for the *y*-axis and the distance between C18 and C78 as the collective variable for the *x*-axis.

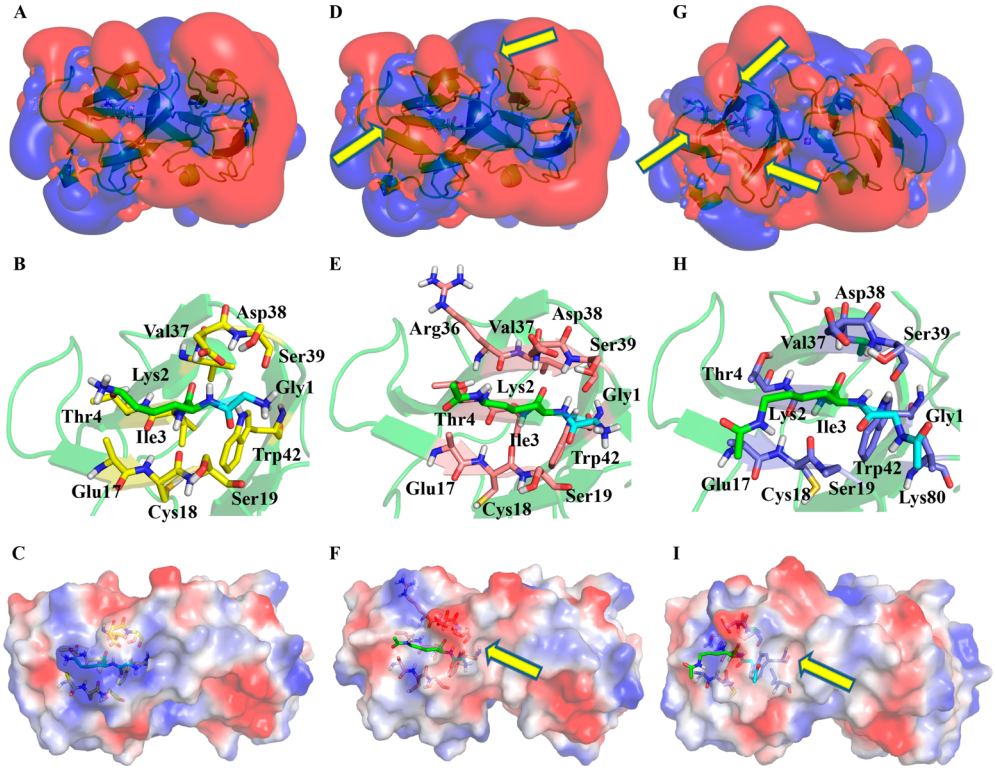

Figure 8. Surface electrostatic potential attributable to acetylation in human γD-crystallin. Molecular electrostatic potential surfaces for nonacetylated (A), K2-acetylated (D), and G1- and K2-acetylated (G) human γD-crystallin that were obtained using the adaptive Poisson−Boltzmann solver. Blue and red contours represent electropositive and electronegative isosurfaces at ±0.3 kT/e, respectively. The residues within a 4-Å radius of K2 (green) and G1 (cyan) are represented as sticks with hydrogens, and hydrogen bonds are represented as red dotted lines (B, E, and H). The vacuum-generated electrostatic potentials near the acetylation region are highlighted in all models, and the models show the electropositive (nonacetylated: C) and electronegative potentials (K2 acetylation: F; G1 and K2 acetylation: I). The yellow arrow in panel D, F, G, and I depicts comparative changes due to acetylation of human γD-crystallin.

dx.doi.org/10.1021/bi501004y | *Biochemistry* 2014, 53, 7269−7282

The associated region that exhibits changes in electropositive and electronegative contours near the acetylation site has been highlighted in Figure 8A,D,G. The relative orientation of the residues in close proximity to K2 (within a ~4-Å radius) and the respective hydrogen bonds (red) are shown in Figure 8B,E,H. Interestingly, as a consequence of acetylation, the surface electronegativity appeared to disperse the electropositive character (blue contours). A similar overview is observed from the vacuum-generated local potential for the proteins (Figure 8C,F,I). On the basis of all of these findings, we concluded that structural perturbations as a result of acetylation promoted thermally induced aggregation of γD-crystallin.

Because lens proteins have a negligible turnover rate throughout the life span, the stability of crystallin proteins is a great concern. Our previous studies on α-crystallin suggested that structural stability modulated its chaperone function. We demonstrated that the enhancement of the chaperone function of α-crystallin under different conditions was commonly associated with increased structural stability.[18,37−39] To determine the effect of acetylation on the structural stability of γD-crystallin, the thermodynamic stability was examined. Equilibrium GdnHCl unfolding was estimated by monitoring the intrinsic tryptophan fluorescence of the protein at various GdnHCl concentrations. The λ_{max} values were recorded at 327 and 355 nm and plotted as a ratio of intensities (I_{327}/I_{355}) against GdnHCl concentration (Figure 9A). A crude estimation of the transition midpoint ($C_{1/2}$) from sigmoidal analysis of the denaturation profiles indicated that the $C_{1/2}$ value decreased from 2.06 M for the nonacetylated protein to 1.77 M of GdnHCl for the acetylated protein (Figure 9A and Table 2). This decrease suggested that acetylation destabilized the overall structural integrity of γD-crystallin. To quantify the stability, all of the profiles were analyzed with the aid of a global three-state fitting procedure, according to the following equation:

$$F = \frac{F_N + F_I \exp(-\Delta G_1^0 + m_1[\text{urea}])/RT + F_U \exp(-\Delta G_2^0 + m_2\cdot[\text{urea}])/RT}{1 + \exp(-\Delta G_1^0 + m_1[\text{urea}])/RT + \exp(-\Delta G_2^0 + m_2\cdot[\text{urea}])/RT} \quad (2)$$

where F_N, F_I, and F_U are the fluorescence intensities for 100% nonacetylated, 100% intermediate, and 100% unfolded forms, respectively. ΔG_1^0 represents the standard free energy change between native (N) and the intermediate (I) forms, and ΔG_2^0 represents the standard free energy change between the I and unfolded (U) forms. ΔG^0, which is the sum of ΔG_1^0 and ΔG_2^0, represents the standard free energy change of unfolding (between the N and U forms) at zero GdnHCl concentration. The standard free energy change of the nonacetylated protein at 37 °C was 41.93 kJ/mol (Table 2). The ΔG^0 value for the acetylated protein was reduced to 35.72 kJ/mol, suggesting a decrease in thermodynamic stability by ~6.21 kJ/mol.

We then compared the stability of the proteins against thermal stress by measuring far-UV CD spectra and the intrinsic tryptophan fluorescence. The change in the ellipticity magnitude at 218 nm (which is characteristic of the β-sheet secondary structure of the protein) and the alteration in the λ_{max} of intrinsic tryptophan fluorescence were monitored over a temperature range from 25 to 90 °C (Figure 9B,C). The thermal denaturation profiles of both proteins were sigmoidal in nature and exhibited an apparent two-state transition. Sigmoidal analysis of far-UV CD profiles demonstrated that the nonacetylated protein underwent thermal unfolding with a midpoint transition or melting temperature (T_m) of 82 °C (Table 3). Acetylation shifted

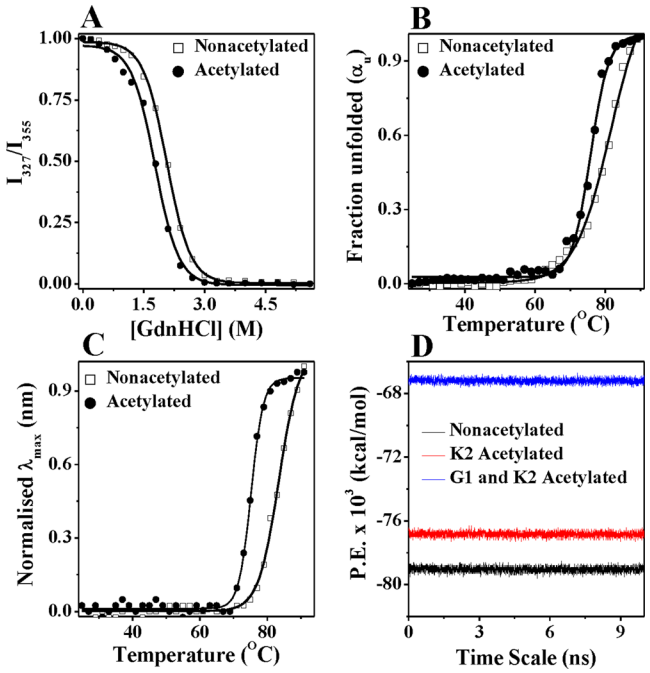

Figure 9. Acetylated γD-crystallin is structurally less stable than the nonacetylated γD-crystallin. Equilibrium GdnHCl unfolding profile for 0.025 mg/mL of nonacetylated and acetylated human γD-crystallin at 37 °C (A). The profile was normalized to a scale of 0−1. Symbols represent the experimental data points, and the solid lines represent the best fit according to the three-state model. The thermal stability of both proteins was evaluated by far-UV CD measurements (B). The temperature was controlled by a water bath, and the data were recorded at a given temperature after a 2 min equilibration. A protein concentration of 0.1 mg/mL in 10 mM phosphate buffer, 5 mM DTT, and 1 mM EDTA (pH 7.0) was used. The raw data were fitted to a two-state model, and the fitting results are represented by solid lines. The thermal stability of both proteins was evaluated by monitoring the intrinsic tryptophan fluorescence (C). The temperature was controlled by a water bath, and the data were recorded at a given temperature after a 2 min equilibration. A protein concentration of 0.025 mg/mL in 10 mM phosphate buffer, 5 mM DTT, and 1 mM EDTA (pH 7.0) was used. The raw data were fitted to a two-state model, and the fitting results are represented by solid lines. Potential energy estimation computed from the molecular dynamics simulation (D). The relative difference in the potential energy profiles indicate the stability of the macro-models in the order nonacetylated > K2-acetylated > G1- and K2-acetylated.

Table 2. $C_{1/2}$ and ΔG^0 Values of Nonacetylated and Acetylated Human γD-Crystallin at 37 °C

protein	$C_{1/2}$ (M)	ΔG^0(kJ/mol)
nonacetylated	2.06 ± 0.04	41.93 ± 0.72
acetylated	1.77 ± 0.05	35.72 ± 0.57

Table 3. Thermal Unfolding Parameters of Nonacetylated and Acetylated Human γD-Crystallin Determined from Far-UV CD Spectroscopy

protein	T_m (°C)
nonacetylated	82.1 ± 0.3
acetylated	75.7 ± 0.4

the T_m value to ~76 °C (Figure 9B and Table 3). A similar decrease in T_m (~8 °C) was also observed when probed using the intrinsic tryptophan fluorescence (Figure 9C, Table 4),

dx.doi.org/10.1021/bi501004y | Biochemistry 2014, 53, 7269−7282

suggesting that acetylation reduced the thermal stability of human γD-crystallin.

Table 4. Thermal Unfolding Parameters of Nonacetylated and Acetylated Human γD-Crystallin Determined from the Intrinsic Tryptophan Fluorescence

protein	T_m (°C)
nonacetylated	83.4 ± 0.5
acetylated	75.2 ± 0.3

We then estimated the structural stability of the nonacetylated and acetylated γD-crystallin by computing the potential energy (PE) of the system throughout the simulation time scale (Figure 9D). The average PE for the nonacetylated protein was found to be -7.9×10^4 kcal/mol, whereas the PE for acetylated K2 and acetylated G1 and K2 was found to be -7.7×10^4 and -6.7×10^4 kcal/mol, respectively. Theoretical analysis, as well as chemical and thermal denaturation experiments, revealed that acetylation significantly decreased the structural stability of human γD-crystallin. A previous study has shown that deamidation, which is another posttranslational modification, also induced a similar reduction in the structural stability of γD-crystallin.[35] In addition, it has been demonstrated that congenital cataract mutants of human γD-crystallin (R14C, G61C) are also structurally less stable than the wild-type protein.[22,40] On the basis of these observations, we concluded that acetylation destabilized human γD-crystallin, which promoted its aggregation under a thermally stressed condition.

In addition to structural stability, lens crystallins exhibit high kinetic stability, which allows them to retain their folded conformation during aging. *In vitro* unfolding/refolding progression of human γD-crystallin has been extensively studied, and these studies indicate that the protein contains a partially folded intermediate population.[41−43] We also examined the effect of acetylation on the unfolding kinetics of γD-crystallin. The increase in tryptophan fluorescence intensity at 355 nm was monitored with time, while the protein was rapidly diluted into 5.5 M GdnHCl (pH 7.0) at 25 °C. The kinetic unfolding profile of the nonacetylated protein was best fit by two exponentials, which suggested the presence of one intermediate (Figure 10A,B). The rate constant values further reflected that the transition of the native state to the intermediate (transition 1) was nearly 10-fold more rapid than the transition from the intermediate to the unfolded state (transition 2) (Table 5). The unfolding transition demonstrated $t_{1/2}$ values of 23.1 and 277 s for the two phases, respectively. The kinetic unfolding transitions for the acetylated protein was best fit by a single exponential with a $t_{1/2}$ value of ~69 s. When we performed this unfolding kinetics experiment at 37 °C, we observed a similar result (data not shown). Collectively, these results revealed that the acetylated protein unfolded more rapidly than the nonacetylated protein.

The effect of acetylation on the refolding kinetics of human γD-crystallin was also determined by productive kinetic refolding experiments at pH 7.0. The protein was diluted from 5.5 M

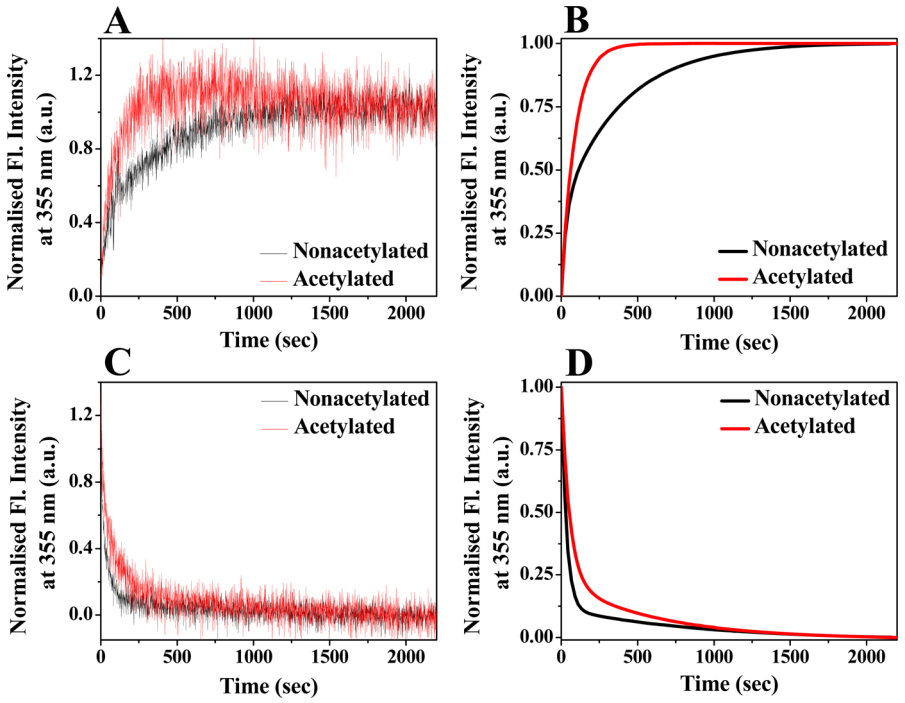

Figure 10. Acetylation alters the unfolding and refolding of γD-crystallin. Productive kinetic unfolding data of nonacetylated and acetylated human γD-crystallin (A). For unfolding, nonacetylated proteins (0.1 mg/mL) were diluted into 5.5 M GdnHCl, 10 mM phosphate buffer, 5 mM DTT, and 1 mM EDTA (pH 7.0) at 25 °C. Changes in the fluorescence intensity at 355 nm were monitored over time using an excitation wavelength of 295 nm. The final protein concentration in the unfolding buffer was 0.01 mg/mL. Unfolding time-course profiles (B) of both proteins were fitted with double and single exponentials, respectively, as indicated by solid lines. Productive kinetic refolding data of nonacetylated and acetylated human γD-crystallin (C). The protein (0.1 mg/mL) was initially unfolded in 5.5 M GdnHCl and diluted into 10 mM phosphate, 5 mM DTT, and 1 mM EDTA (pH 7.0) at 25 °C to yield a final GdnHCl concentration of 1.0 M. The final protein concentration was 0.01 mg/mL. Changes in the fluorescence intensity at 355 nm were monitored over time using an excitation wavelength of 295 nm. Both refolding time-course profiles were fitted with double exponentials, as indicated by solid lines (D).

dx.doi.org/10.1021/bi501004y | *Biochemistry* 2014, 53, 7269−7282

Table 5. Productive Kinetic Unfolding Parameters of Nonacetylated and Acetylated Human γD-Crystallin

	kinetic unfolding transition 1		kinetic unfolding transition 2	
protein	k_1 (s^{-1})	$t^1_{1/2}$ (s)	k_2 (s^{-1})	$t^2_{1/2}$ (s)
nonacetylated	0.03 ± 0.004	23.1 ± 3.0	0.0025 ± 0.0001	277 ± 9
acetylated	0.01 ± 0.001	69.3 ± 6.0		

Table 6. Productive Kinetic Refolding Parameters of Nonacetylated and Acetylated Human γD-Crystallin

	kinetic refolding transition 1		kinetic refolding transition 2	
protein	k_1(s^{-1})	$t^1_{1/2}$(s)	k_2(s^{-1})	$t^2_{1/2}$ (s)
nonacetylated	0.07 ± 0.003	9.9 ± 0.5	0.0083 ± 0.0003	83.5 ± 0.5
acetylated	0.02 ± 0.001	34.6 ± 1.0	0.0016 ± 0.0001	433.1 ± 3.0

GdnHCl to 1.0 M GdnHCl, and the decrease in intrinsic tryptophan fluorescence intensity at 355 nm was monitored (Figure 10C,D). The refolding kinetics profile of the nonacetylated protein exhibited a rapid decrease in fluorescence intensity up to 180 s followed by a gradual decrease during the remainder of the assay. The profile was best fit by two exponentials (Figure 10D), yielding $t_{1/2}$ values of 9.9 and 83.5 s for the unfolded state (U) → intermediate state (I) (transition 1) and intermediate (I) → native state (N) (transition 2), respectively (Table 6). The $t_{1/2}$ values for the U → I and I → N transitions increased ∼4- to 5-fold for the acetylated protein compared with that of the nonacetylated protein (Table 6), suggesting that refolding of the acetylated protein was slower than the nonacetylated protein. The results obtained from structural stability and unfolding/refolding kinetics experiments suggested that G1 and K2 in the N-terminal region of γD-crystallin are critical for both the overall structural stability and the kinetic stability of this protein. Our results are analogous to previous observations that deamidation and cataract-causing point mutations in the N-terminal region of γD-crystallin (L5S, V75D) decreased the kinetic unfolding barrier of γD-crystallin.[35,41] Interestingly, our results also demonstrate that acetylation destabilized the native conformation by decreasing the potential barrier of the unfolding pathway, which may be account for the increased aggregation of the acetylated protein under thermal stress.

Folding studies of multidomain proteins are of significant importance. The geometry of interdomain interfaces and stability of different domains play a crucial role in protein folding. Partially unfolded chains/domains are often known to trigger aggregation reactions, which in turn lead to several protein aggregation diseases.[44] Human γD-crystallin has two indistinct domains (N- and C-terminal domains). Although, acetylation of G1 and K2 residues in the N-terminal domain of this protein grossly perturbed the tertiary structure, structural stability and cysteine microenvironment, negligible alteration in the secondary structure of this protein indicated that only a part of the protein is involved for such alteration. Moreover, theoretical studies also predicted that acetylation of γD-crystallin brought the two distant cysteine residues (C18 and C78) in the N-terminal domain within close proximity of each other. In light of all these observations, it appeared acetylation affected the stability of the two domains in human γD-cystallin. Previously, several attempts have been made to understand the folding and stability of these two domains in this crystallin protein using unfolding/refolding kinetic experiments.[6,41,45] All these studies used an assumption/hypothesis proposed by Flaugh et al. during analyzing the data associated with these experiments i.e. during unfolding/refolding kinetics experiment, the native to intermediate transition corresponds to unfolding/refolding of N-terminal domain and the intermediate to unfolded transition corresponds to unfolding/refolding of the C- terminal domain of γD-crystallin.[41] We also used this hypothesis to understand the effect of acetylation on the stability of these two domains in human γD-crystallin. When the kinetic unfolding profile of nonacetylated and acetylated γD-crystallin was compared, it was found that the N-terminal domain of the acetylated protein unfolded faster than that of the nonacetylated protein (Table 5). When the kinetic refolding profiles of both the proteins were compared, it was found that the N-terminal domain of the acetylated protein takes longer time to refold compared to the nonacetylated protein. However, when the same was compared for the C-terminal domain, the difference in refolding time for these two proteins was comparatively less (Table 6). Therefore, we can suggest that acetylation of human γD-crystallin presumably destabilized its N-terminal domain more compared to its C-terminal domain which made γD-crystallin more prone to aggregation (Figure 3B).

Our biophysical studies clearly revealed that the structural stability of γD-crystallin was decreased due to acetylation, which was accompanied by a perturbed tertiary structure and native-like secondary structure. This finding led us to hypothesize that acetylation of γD-crystallin may induce the formation of a molten globule-like intermediate structure. The term "molten globule" evolved from the work of Ohgushi and Wada in 1983.[46] A molten globule is typically an intermediate state, which is clearly different from the native and denatured states of a protein, with a native-like secondary structure but grossly perturbed/disordered tertiary structure and a significant exposure of hydrophobic surface. Chemical modifications of proteins are often responsible for the formation of a molten globule structure. For example, reductive alkylation of lysine residues induced a molten globule structure in the thermostable lipase found in the *Geobacillus zalihae* strain T1 and decreased the stability of this protein.[47] Another example is the modification of ε-amino groups of lysine residues in glucose oxidase, which resulted in a molten globule-like intermediate structure of the protein.[48] These studies also demonstrated that the partially flexible structure of the molten globule-like intermediate state exposed a higher amount of hydrophobic sites on its surface. Therefore, we evaluated whether acetylation exposed hydrophobic sites in γD-crystallin using bis-ANS as a hydrophobic probe. This hydrophobic probe is commonly used to monitor the molten globule state in a protein.[49,50] We observed that the fluorescence intensity of bis-ANS bound to the protein was ∼30% higher compared with the nonacetylated protein (Figure 11). This finding suggested that acetylation induced a molten globule state in γD-crystallin with a semiflexible structure, which permitted exposure of some hydrophobic groups at the protein surface. This probably led

dx.doi.org/10.1021/bi501004y | *Biochemistry* 2014, 53, 7269−7282

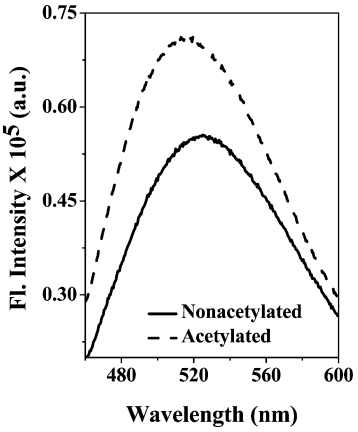

Figure 11. Acetylation exposes additional hydrophobic sites at the surface of γD-crystallin. The concentrations of the protein samples and bis-ANS were 2.5 μM and 10 μM, respectively. All samples were prepared in 10 mM phosphate buffer, 5 mM DTT, and 1 mM EDTA (pH 7.0). The fluorescence spectrum of bis-ANS bound to different samples was recorded from 450 to 600 nm at 25 °C. The excitation wavelength was 390 nm.

to the increase in aggregation of γD-crystallin under thermal stress.

In summary, the present study has demonstrated that G1 and K2 acetylation occurred in γD-crystallin of the human lens and that this acetylation decreased the structural stability, altered the unfolding/refolding kinetics, and perturbed the conformation of this protein. Whether the acetylation of γD-crystallin alters the binding affinity of γD-crystallin for α-crystallin remains to be determined. We propose that these changes increase the propensity of γD-crystallin to self-aggregate and contribute to the aggregation of proteins that occurs in aging and cataractous lenses.

■ ASSOCIATED CONTENT

Supporting Information

Sequence alignment to show conserved K2 in human γ-crystallin variants. This material is available free of charge via the Internet at http://pubs.acs.org.

■ AUTHOR INFORMATION

Corresponding Authors

*(R.N.) Phone: 303-724-5922. Fax: 303-724-5270. E-mail: ram.nagaraj@ucdenver.edu.

*(A.B.) Phone: +91-674-2576051. Fax: +91-674-2306202. E-mail: abiswas@iitbbs.ac.in.

Present Address

[‖]Department of Ophthalmology, University of Colorado School of Medicine, 12800 East 19th Avenue, RC-1 North 5102, Aurora CO 80045.

Author Contributions

[#]M.A.D. and S.K.N. contributed equally to this work.

Notes

The authors declare no competing financial interest.

■ ACKNOWLEDGMENTS

This study was supported by National Institutes of Health Grants R01EY-022061, R01EY-023286 (R.H.N.), P30EY-11373 (Visual Sciences Research Center of Case Western Reserve University), Research to Prevent Blindness, NY, The Ohio Lions Eye Research Foundation and the CSIR India Grant 37(1535)/12/EMR-II (AB). S.K.N. acknowledges the receipt of an Institute Fellowship from the Indian Institute of Technology Bhubaneswar. We thank Drs. Rooban Nahomi and Sruthi Sampathkumar for critical reading of the manuscript.

■ ABBREVIATIONS

bis-ANS, 4,4′-dianilino-1,1′-binaphthyl-5,5′-disulfonic acid, dipotassium salt; DTNB, 5,5′-dithiobis(2-nitrobenzoic acid); TNB, 2-nitro-5-thiobenzoic acid; DTT, dithiothreitol; GdnHCl, guanidine hydrochloride; MD, molecular dynamics; APBS, adaptive Poisson−Boltzmann solver

■ REFERENCES

(1) Bloemendal, H. (1982) Lens proteins. *CRC Crit. Rev. Biochem. 12*, 1−38.

(2) Benedek, G. B. (1971) Theory of transparency of the eye. *Appl. Opt. 10*, 459−473.

(3) Delaye, M., and Tardieu, A. (1983) Short-range order of Crystallin proteins accounts for eye lens transparency. *Nature 302*, 415−417.

(4) Bron, A. J., Vrensen, G. F., Koretz, J., Maraini, G., and Harding, J. J. (2000) The ageing lens. *Ophthalmologica 214*, 86−104.

(5) Horwitz, J. (1992) Alpha-Crystallin can function as a molecular chaperone. *Proc. Natl. Acad. Sci. U. S. A. 89*, 10449−10453.

(6) Flaugh, S. L., Kosinski-Collins, M. S., and King, J. (2005) Interdomain side-chain interactions in human gammaD Crystallin influencing folding and stability. *Protein Sci. 14*, 2030−2043.

(7) Basak, A., Bateman, O., Slingsby, C., Pande, A., Asherie, N., Ogun, O., Benedek, G. B., and Pande, J. (2003) High-resolution X-ray crystal structures of human gammaD Crystallin (1.25 Å) and the R58H mutant (1.15 Å) associated with aculeiform cataract. *J. Mol. Biol. 328*, 1137−1147.

(8) Sharma, K. K., and Santhoshkumar, P. (2009) Lens aging: effects of crystallins. *Biochim. Biophys. Acta 1790*, 1095−1108.

(9) Park, Z. I., Sadygov, R., Clark, M. J., ClarkI, J., and Yates, J. R. (2007) Assigning in vivo carbamylation and acetylation in human lens proteins using tandem mass spectrometry and database searching. *Int. J. Mass Spectrom. 259*, 161−173.

(10) Hanson, S. R., Hasan, A., Smith, D. L., and Smith, J. B. (2000) The major in vivo modifications of the human water-insoluble lens crystallins are disulfide bonds, deamidation, methionine oxidation and backbone cleavage. *Exp. Eye Res. 71*, 195−207.

(11) Lampi, K. J., Ma, Z., Shih, M., Shearer, T. R., Smith, J. B., Smith, D. L., and David, L. L. (1997) Sequence analysis of betaA3, betaB3, and betaA4 crystallins completes the identification of the major proteins in young human lens. *J. Biol. Chem. 272*, 2268−2275.

(12) Hanson, S. R., Smith, D. L., and Smith, J. B. (1998) Deamidation and disulfide bonding in human lens gamma-crystallins. *Exp. Eye Res. 67*, 301−312.

(13) Searle, B. C., Dasari, S., Wilmarth, P. A., Turner, M., Reddy, A. P., David, L. L., and Nagalla, S. R. (2005) Identification of protein modifications using MS/MS de novo sequencing and the OpenSea alignment algorithm. *J. Proteome Res. 4*, 546−554.

(14) Lapko, V. N., Smith, D. L., and Smith, J. B. (2003) Methylation and carbamylation of human gamma-crystallins. *Protein Sci. 12*, 1762−1774.

(15) Polevoda, B., and Sherman, F. (2003) N-terminal acetyltransferases and sequence requirements for N-terminal acetylation of eukaryotic proteins. *J. Mol. Biol. 325*, 595−622.

(16) Sadoul, K., Wang, J., Diagouraga, B., and Khochbin, S. (2011) The tale of protein lysine acetylation in the cytoplasm. *J. Biomed. Biotechnol. 2011*, 970382.

(17) Choudhary, C., Weinert, B. T., Nishida, Y., Verdin, E., and Mann, M. (2014) The growing landscape of lysine acetylation links metabolism and cell signalling. *Nat. Rev. Mol. Cell Biol. 15*, 536−550.

(18) Nagaraj, R. H., Nahomi, R. B., Shanthakumar, S., Linetsky, M., Padmanabha, S., Pasupuleti, N., Wang, B., Santhoshkumar, P., Panda, A.

K., and Biswas, A. (2012) Acetylation of alphaA-Crystallin in the human lens: effects on structure and chaperone function. *Biochim. Biophys. Acta 1822*, 120−129.
(19) Nahomi, R. B., Oya-Ito, T., and Nagaraj, R. H. (2013) The combined effect of acetylation and glycation on the chaperone and anti-apoptotic functions of human alpha-Crystallin. *Biochim. Biophys. Acta 1832*, 195−203.
(20) Nahomi, R. B., Huang, R., Nandi, S. K., Wang, B., Padmanabha, S., Santhoshkumar, P., Filipek, S., Biswas, A., and Nagaraj, R. H. (2013) Acetylation of Lysine92 Improves the Chaperone and Anti-apoptotic Activities of Human alphaB-Crystallin. *Biochemistry 52*, 8126−8138.
(21) Das, K. P., and Surewicz, W. K. (1995) Temperature-induced exposure of hydrophobic surfaces and its effect on the chaperone activity of alpha-Crystallin. *FEBS Lett. 369*, 321−325.
(22) Pande, A., Pande, J., Asherie, N., Lomakin, A., Ogun, O., King, J. A., Lubsen, N. H., Walton, D., and Benedek, G. B. (2000) Molecular basis of a progressive juvenile-onset hereditary cataract. *Proc. Natl. Acad. Sci. U. S. A. 97*, 1993−1998.
(23) Provencher, S. W., and Glockner, J. (1981) Estimation of globular protein secondary structure from circular dichroism. *Biochemistry 20*, 33−37.
(24) Nandi, S. K., Rehna, E. A., Panda, A. K., Shiburaj, S., Dharmalingam, K., and Biswas, A. (2013) A S52P mutation in the 'alpha-Crystallin domain' of Mycobacterium leprae HSP18 reduces its oligomeric size and chaperone function. *FEBS J. 280*, 5994−6009.
(25) Jorgensen, W. L., Maxwell, D. S., and TiradoRives, J. (1996) Development and testing of the OPLS all-atom force field on conformational energetics and properties of organic liquids. *J. Am. Chem. Soc. 118*, 11225−11236.
(26) Dolinsky, T. J., Nielsen, J. E., McCammon, J. A., and Baker, N. A. (2004) PDB2PQR: an automated pipeline for the setup of Poisson-Boltzmann electrostatics calculations. *Nucleic Acids Res. 32*, W665−667.
(27) Krautler, V., Van Gunsteren, W. F., and Hunenberger, P. H. (2001) A fast SHAKE: Algorithm to solve distance constraint equations for small molecules in molecular dynamics simulations. *J. Comput. Chem. 22*, 501−508.
(28) Tuckerman, M., Berne, B. J., and Martyna, G. J. (1992) Reversible Multiple Time Scale Molecular-Dynamics. *J. Chem. Phys. 97*, 1990−2001.
(29) Zarina, S., Abbasi, A., and Zaidi, Z. H. (1992) Primary structure of beta s-Crystallin from human lens. *Biochem. J. 287* (Pt 2), 375−381.
(30) Andley, U. P. (2006) Crystallins and hereditary cataracts: molecular mechanisms and potential for therapy. *Expert Rev. Mol. Med. 8*, 1−19.
(31) Fujii, N., Hiroki, K., Matsumoto, S., Masuda, K., Inoue, M., Tanaka, Y., Awakura, M., and Akaboshi, M. (2001) Correlation between the loss of the chaperone-like activity and the oxidation, isomerization and racemization of gamma-irradiated alpha-Crystallin. *Photochem. Photobiol. 74*, 477−482.
(32) Ito, H., Kamei, K., Iwamoto, I., Inaguma, Y., Nohara, D., and Kato, K. (2001) Phosphorylation-induced change of the oligomerization state of alpha B-Crystallin. *J. Biol. Chem. 276*, 5346−5352.
(33) Gupta, R., and Srivastava, O. P. (2004) Deamidation affects structural and functional properties of human alphaA-Crystallin and its oligomerization with alphaB-Crystallin. *J. Biol. Chem. 279*, 44258−44269.
(34) Nagaraj, R. H., Oya-Ito, T., Padayatti, P. S., Kumar, R., Mehta, S., West, K., Levison, B., Sun, J., Crabb, J. W., and Padival, A. K. (2003) Enhancement of chaperone function of alpha-Crystallin by methylglyoxal modification. *Biochemistry 42*, 10746−10755.
(35) Flaugh, S. L., Mills, I. A., and King, J. (2006) Glutamine deamidation destabilizes human gammaD-Crystallin and lowers the kinetic barrier to unfolding. *J. Biol. Chem. 281*, 30782−30793.
(36) Schafheimer, N., and King, J. (2013) Tryptophan cluster protects human gammaD-Crystallin from ultraviolet radiation-induced photoaggregation in vitro. *Photochem. Photobiol. 89*, 1106−1115.
(37) Biswas, A., and Das, K. P. (2004) Role of ATP on the interaction of alpha-Crystallin with its substrates and its implications for the molecular chaperone function. *J. Biol. Chem. 279*, 42648−42657.
(38) Biswas, A., Goshe, J., Miller, A., Santhoshkumar, P., Luckey, C., Bhat, M. B., and Nagaraj, R. H. (2007) Paradoxical effects of substitution and deletion mutation of Arg56 on the structure and chaperone function of human alphaB-Crystallin. *Biochemistry 46*, 1117−1127.
(39) Nagaraj, R. H., Panda, A. K., Shanthakumar, S., Santhoshkumar, P., Pasupuleti, N., Wang, B., and Biswas, A. (2012) Hydroimidazolone modification of the conserved Arg12 in small heat shock proteins: studies on the structure and chaperone function using mutant mimics. *PLoS One 7*, e30257.
(40) Zhang, W., Cai, H. C., Li, F. F., Xi, Y. B., Ma, X., and Yan, Y. B. (2011) The congenital cataract-linked G61C mutation destabilizes gammaD-Crystallin and promotes non-native aggregation. *PLoS One 6*, e20564.
(41) Flaugh, S. L., Kosinski-Collins, M. S., and King, J. (2005) Contributions of hydrophobic domain interface interactions to the folding and stability of human gammaD-Crystallin. *Protein Sci. 14*, 569−581.
(42) Kosinski-Collins, M. S., Flaugh, S. L., and King, J. (2004) Probing folding and fluorescence quenching in human gammaD Crystallin Greek key domains using triple tryptophan mutant proteins. *Protein Sci. 13*, 2223−2235.
(43) Kosinski-Collins, M. S., and King, J. (2003) In vitro unfolding, refolding, and polymerization of human gammaD Crystallin, a protein involved in cataract formation. *Protein Sci. 12*, 480−490.
(44) Dobson, C. M. (2004) Principles of protein folding, misfolding and aggregation. *Semin. Cell Dev. Biol. 15*, 3−16.
(45) Moreau, K. L., and King, J. (2009) Hydrophobic core mutations associated with cataract development in mice destabilize human gammaD-Crystallin. *J. Biol. Chem. 284*, 33285−33295.
(46) Ohgushi, M., and Wada, A. (1983) 'Molten-globule state': a compact form of globular proteins with mobile side-chains. *FEBS Lett. 164*, 21−24.
(47) Cheong, K. W., Leow, T. C., Rahman, R. N., Basri, M., Rahman, M. B., and Salleh, A. B. (2011) Reductive alkylation causes the formation of a molten globule-like intermediate structure in Geobacillus zalihae strain T1 thermostable lipase. *Appl. Biochem. Biotechnol. 164*, 362−375.
(48) Hosseinkhani, S., Ranjbar, B., Naderi-Manesh, H., and Nemat-Gorgani, M. (2004) Chemical modification of glucose oxidase: possible formation of molten globule-like intermediate structure. *FEBS Lett. 561*, 213−216.
(49) Shi, L., Palleros, D. R., and Fink, A. L. (1994) Protein conformational changes induced by 1,1′-bis(4-anilino-5-naphthalene-sulfonic acid): preferential binding to the molten globule of DnaK. *Biochemistry 33*, 7536−7546.
(50) Brumano, M. H., and Oliveira, M. G. (2004) Urea-induced denaturation of beta-trypsin: an evidence for a molten globule state. *Protein Pept. Lett. 11*, 133−140.